

Carrier-Doping Dependence of Critical Current Density in $\text{Ba}_{1-x}\text{K}_x\text{Fe}_2\text{As}_2$ Single Crystals and Superconducting Wires

S Pyon, T Suwa, and T Tamegai

Department of Applied Physics, The University of Tokyo, Hongo, Bunkyo-ku, Tokyo 113-8656, Japan

E-mail: pyon@ap.t.u-tokyo.ac.jp

Abstract. The carrier-doping dependence of J_c in $\text{Ba}_{1-x}\text{K}_x\text{Fe}_2\text{As}_2$ single crystals and superconducting wires were investigated. $\text{Ba}_{1-x}\text{K}_x\text{Fe}_2\text{As}_2$ single crystals ($0.24 < x < 0.4$) are synthesized by commonly used FeAs self-flux method, while $\text{Ba}_{1-x}\text{K}_x\text{Fe}_2\text{As}_2$ wires are fabricated by powder-in-tube (PIT) method and hot isostatic pressing (HIP) technique, using polycrystalline $\text{Ba}_{1-x}\text{K}_x\text{Fe}_2\text{As}_2$ ($0.25 < x < 0.4$) prepared by solid state reaction and silver and copper tubes. Their magnetic J_c was characterized by magnetization measurements. We found that the x -dependence of J_c in single crystals shows the peak in under-doped region around $x \sim 0.28$ similar to previous study. In the HIP wire, although significant peak is not observed, J_c shows a broad plateau in a wide doping region of $0.3 < x < 0.4$. These results indicate that J_c in the under-doped $\text{Ba}_{1-x}\text{K}_x\text{Fe}_2\text{As}_2$ HIP wire is controlled by intergranular J_c .

1. Introduction

Iron-based superconductors (IBSs) are promising candidates for high-field applications of superconductors because they exhibit high critical temperature T_c , large upper critical field H_{c2} , and relatively low anisotropy compared with cuprate superconductors. Among them, $A_{1-x}\text{K}_x\text{Fe}_2\text{As}_2$ ($A = \text{Ba}, \text{Sr}$) compounds (122-type) are considered to be most attractive candidates. They have small anisotropies of 2-3, moderate T_c 's, large H_{c2} 's, and large J_c 's [1-2]. Actually high critical current density is realized in superconducting wires or tapes using $A_{1-x}\text{K}_x\text{Fe}_2\text{As}_2$ [3-10]. In these report, K content x in the starting materials for superconducting wires and tapes are fixed to 0.4, where T_c is optimized [11,12]. Recently, however, Song *et al.* reported distinct doping dependence of J_c and T_c in $\text{Ba}_{1-x}\text{K}_x\text{Fe}_2\text{As}_2$ single crystals, which were synthesized by KAs self-flux method [13]. The x -dependence of J_c is characterized by a peak at $x = 0.3$, which corresponds to the under-doped region. The origin of the characteristic doping dependence of J_c may be connected with the pinning forces related to the orthorhombic phase domain boundary or to the chemical inhomogeneity introduced by the dopant substitutions [13]. This result implies that higher J_c may also be achieved not at the optimal-doping level of $x \sim 0.4$ for T_c but at under-doped region in 122-type superconducting wires and tapes. However, to our knowledge, there have been no systematic studies on the x -dependence of J_c in $\text{Ba}_{1-x}\text{K}_x\text{Fe}_2\text{As}_2$ wires and tapes. Furthermore, we were also interested in the investigation of x -dependence of J_c in $\text{Ba}_{1-x}\text{K}_x\text{Fe}_2\text{As}_2$ single crystals synthesized by commonly used FeAs self-flux method, since the process of crystal growth should affect chemical homogeneities which generate pinning forces.

In this work, we focused on carrier-doping dependence of J_c in $\text{Ba}_{1-x}\text{K}_x\text{Fe}_2\text{As}_2$ single crystals and superconducting wires. Single crystals are synthesized by FeAs flux method. And superconducting wires were fabricated by powder-in-tube (PIT) method using well characterized $\text{Ba}_{1-x}\text{K}_x\text{Fe}_2\text{As}_2$



polycrystalline powders. J_c and T_c in prepared samples were evaluated from magnetization measurements.

2. Experiment

Single crystals of $(\text{Ba,K})\text{Fe}_2\text{As}_2$ were synthesized by self-flux method using FeAs flux. We used Ba pieces, K ingots and FeAs powder as starting materials. FeAs was prepared by placing stoichiometric amounts of As pieces and Fe powder in an evacuated quartz tube and reacting them at 700°C for 40 h after heating them at 500°C for 10 h. A mixture with a ratio of $\text{Ba}:\text{K}:\text{FeAs} = 1-x:1.1x:4$ was placed in an alumina crucible and sealed in a stainless steel containers [14] in a nitrogen-filled glove box. In order to compensate the loss of elements, 10% excess K was added. They were heated for 1 h at $1200\sim 1250^\circ\text{C}$ followed by cooling down to 900°C at a rate of $5^\circ\text{C}/\text{h}$. Obtained single crystals were separated from flux and cut into rectangular shape as shown in fig.1(a). In order to characterize the compositions of pieces of single crystals, a scanning electron microscope equipped with an energy-dispersive x-ray spectroscopy (SEM-EDX) was used (S-4300, Hitachi High-Technologies equipped with EMAX x-act, HORIBA). Bulk magnetization was measured by a superconducting quantum interference device (SQUID) magnetometer (MPMS-5XL, Quantum Design).

$(\text{Ba,K})\text{Fe}_2\text{As}_2$ superconducting wires were fabricated by ex-situ PIT method. Polycrystalline powders of $\text{Ba}_{1-x}\text{K}_x\text{Fe}_2\text{As}_2$ were prepared by the solid-state reaction. Ba pieces, K ingots, Fe powder, and As pieces were used as starting materials. In order to compensate the loss of elements, the starting mixture contained 15% excess K and 5% excess As. They were mixed in a nitrogen atmosphere more than 10 hour using a ball-milling machine and densely packed into a niobium tube. The niobium tube was then put into a stainless steel tube and sealed in nitrogen filled glove box for heat treatment at 900°C for 30 h. The surface of the obtained polycrystalline ingot was polished to remove small impurities. It was then ground into powder using an agate mortar in nitrogen filled glove box. The phase identification of the sample was carried out by means of powder x-ray diffraction (XRD) with Cu-K α radiation (Smartlab, Rigaku). Ground powders were filled in a silver tube with an outer diameter of 4.5 mm and an inner diameter 3 mm, then cold drawn into a square shape with a diagonal dimension of ~ 1.2 mm. After cutting it into short pieces, one of the pieces was put into 1/8 inch copper tube and redrawn down to the diagonal dimension of 1.2 mm. After that, both ends of the wires were sealed by using an arc furnace. The sealed wires were sintered using the hot isostatic pressing (HIP) technique. Wires and tapes were heated for 0.5 h at 700°C in argon atmosphere under the pressure of 9 MPa. An optical micrograph of the cross section of the HIP wire is shown in fig. 1(b). Bulk magnetization was measured by the same method and intergranular J_c was evaluated using the extended Bean model.

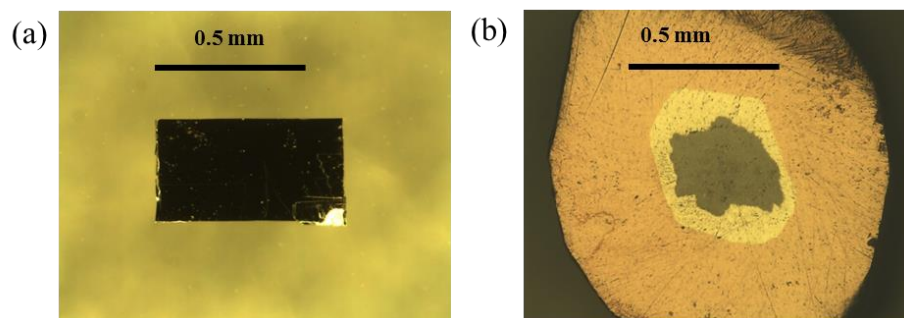


Figure 1. Optical micrographs of typical $\text{Ba}_{1-x}\text{K}_x\text{Fe}_2\text{As}_2$ (a) single crystal and (b) HIP wire, respectively.

3. Results and Discussion

Before the fabrication of wires, polycrystalline powders of $\text{Ba}_{1-x}\text{K}_x\text{Fe}_2\text{As}_2$ were characterized by magnetization and powder x-ray diffraction measurements. Fig. 2(a) shows the temperature dependence of magnetization of several $\text{Ba}_{1-x}\text{K}_x\text{Fe}_2\text{As}_2$ polycrystalline powders with x from 0.25 to 0.40. All the samples show bulk superconductivity. While diamagnetism starts at ~ 38 K in all the

sample, the magnetization curves of under-doped samples show broad drop, especially in $x \sim 0.25$. These broadenings indicate the distribution of carrier concentration in polycrystalline powders. Considering the superconducting dome in $\text{Ba}_{1-x}\text{K}_x\text{Fe}_2\text{As}_2$ phase diagram [11], broadening of the superconducting transition caused by the distribution of carrier contents should become wider at under-doped region. It should be noted that no impurity phases are detected in the x-ray diffraction pattern of these powders. As shown in fig. 2(b), (0 0 2) powder x-ray diffraction peaks of several $\text{Ba}_{1-x}\text{K}_x\text{Fe}_2\text{As}_2$ powders shows the systematic shift. These results suggest that obtained polycrystalline powders are single phases, respectively, and carrier content of x is systematically controlled. Using these powders, HIP wires were fabricated.

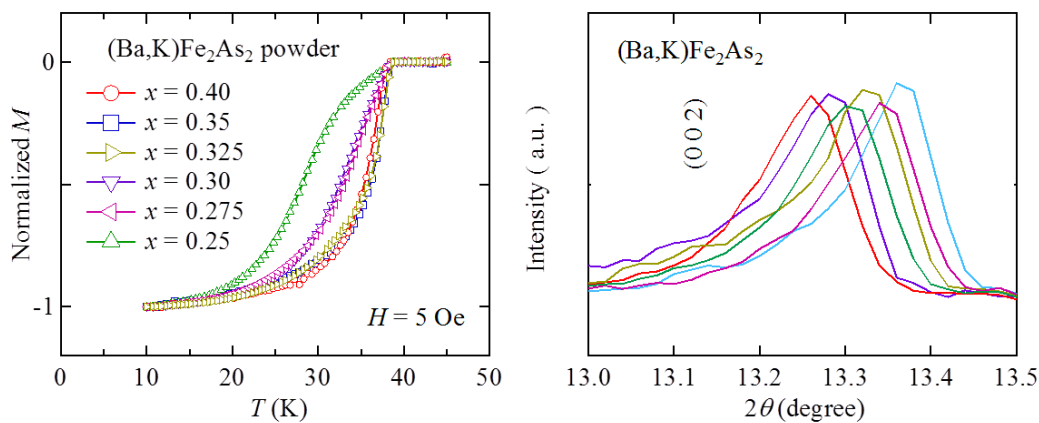


Figure 2. (a) Temperature dependence of magnetization of several $\text{Ba}_{1-x}\text{K}_x\text{Fe}_2\text{As}_2$ polycrystalline powders. (b) Normalized (0 0 2) powder x-ray diffraction peak of several $\text{Ba}_{1-x}\text{K}_x\text{Fe}_2\text{As}_2$ powders.

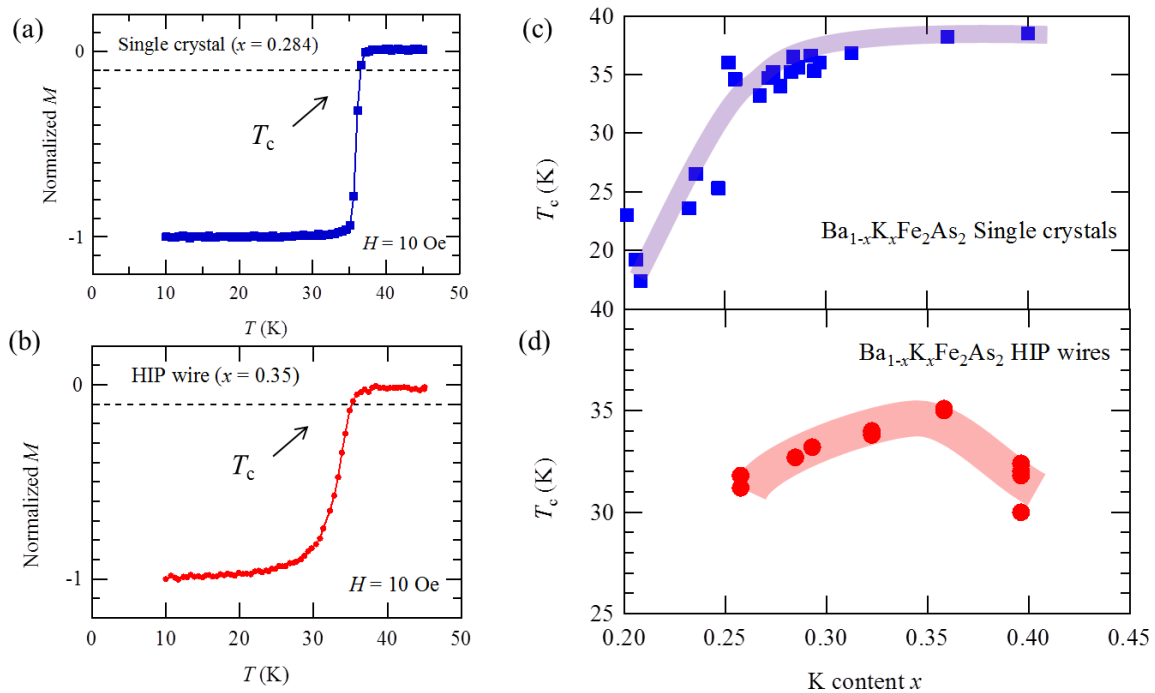


Figure 3. Typical temperature dependence of magnetizations of several $\text{Ba}_{1-x}\text{K}_x\text{Fe}_2\text{As}_2$ (a) single crystal and (b) HIP wire, respectively. K content dependence of T_c in several $\text{Ba}_{1-x}\text{K}_x\text{Fe}_2\text{As}_2$ (c) single crystals and (d) HIP wires, respectively. T_c is defined at the temperature where normalized magnetization reaches at -0.1 as shown in (a) and (b).

To evaluate the carrier-concentration dependence of superconducting properties, such as T_c and J_c , K content of samples should be estimated. From SEM-EDX analyses, the chemical compositions in single crystal and the core of HIP wires were evaluated. In the case of HIP wire, nominal and analyzed carrier contents are almost identical. In the case of single crystals, analyzed K content x is quite different from the nominal value in some pieces. For example, analyzed carrier content in single crystals with nominal carrier content $x \sim 0.28$ are distributed in the range of $0.20 < x < 0.30$. So we perform EDX analysis for each single crystal before evaluating its T_c and J_c .

Next, we evaluate T_c in both single crystals and HIP wires from temperature dependence of magnetization. Typical temperature dependence of magnetization are shown in fig. 3 (a) and (b). Similar to magnetization of polycrystalline powders in fig.2, drop of magnetization tends to be broad in under-doped samples. In this study, T_c is defined at the temperature where normalized magnetization reaches at -0.1 as shown in fig. 3 (a) and (b). Evaluated T_c of single crystals and HIP wires are summarized in fig. 3(c) and (d), respectively. T_c in single crystals is the highest at $x \sim 0.4$. This is consistent with the previous reports. T_c is reduced with decreasing x moderately above $x \sim 0.3$, and rapidly below $x \sim 0.3$. In the HIP wires, x -dependence of T_c shows a broad peak.

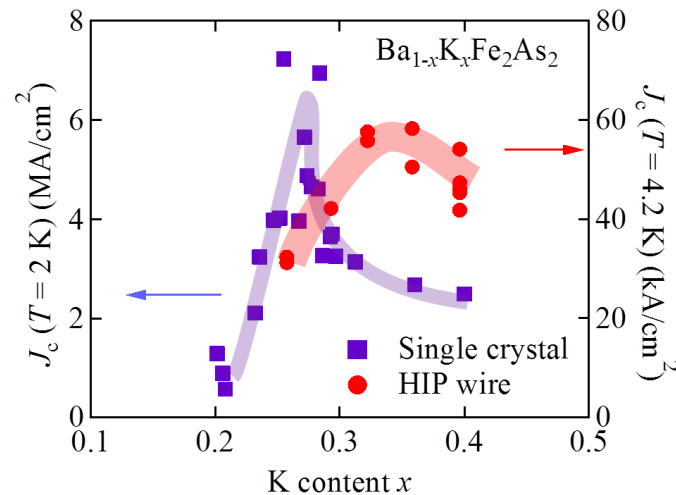


Figure 4. K content dependence of J_c in several $\text{Ba}_{1-x}\text{K}_x\text{Fe}_2\text{As}_2$ single crystals and HIP wires. J_c in self field is evaluated at 2 K and 4.2 K for single crystals and for the HIP wires, respectively.

Magnetic J_c in all of these single crystals and HIP wires are evaluated. Obtained results are summarized in fig.4. J_c in self field is evaluated at 2 K and 4.2 K for single crystals and for the HIP wires, respectively. Maximum of J_c in single crystals reaches around 5-7 MA/cm² at $x \sim 0.28$. This is relatively high value compared with the J_c at $x \sim 0.4$ where T_c is optimized as shown in fig. 3. In our sample grown by FeAs flux method, J_c takes its maximum in the under-doped region. This result is roughly consistent with previous report by Song *et al.*, where KAs flux was used [13], although the peak position is not $x \sim 0.30$. This difference may be caused by the difference in the starting materials for synthesis. In the case of x dependence of J_c in the HIP wire, significant peak is not observed at $x \sim 0.28$. However, J_c shows a broad plateau in a wide doping region of $0.3 < x < 0.4$. J_c is reduced only below $x \sim 0.30$. We can safely conclude that the shift of maximum of J_c from optimal region to under-doped region is the common feature in 122-type single crystals and wires.

In fig. 5, K content dependences of both T_c and J_c in several $\text{Ba}_{1-x}\text{K}_x\text{Fe}_2\text{As}_2$ HIP wires are shown. Both dependences show broad peaks around $x \sim 0.35$. In contrast to the doping dependence of T_c and J_c in single crystals, maximum values are realized in almost the same doping level, although the peak is shifted to under-doped region. This fact suggests that intergranular J_c is dominant compared with intragranular J_c in the core of the HIP wire. Furthermore, sintering conditions for wires and tapes using

under-doped polycrystalline powders have not been well studied yet. In this sense, J_c in 122-type superconducting wires and tapes may further be enhanced by controlling the carrier content and the optimization of sintering process. Obtained results will expand the doping level of starting materials for IBS high- J_c superconducting wires and tapes.

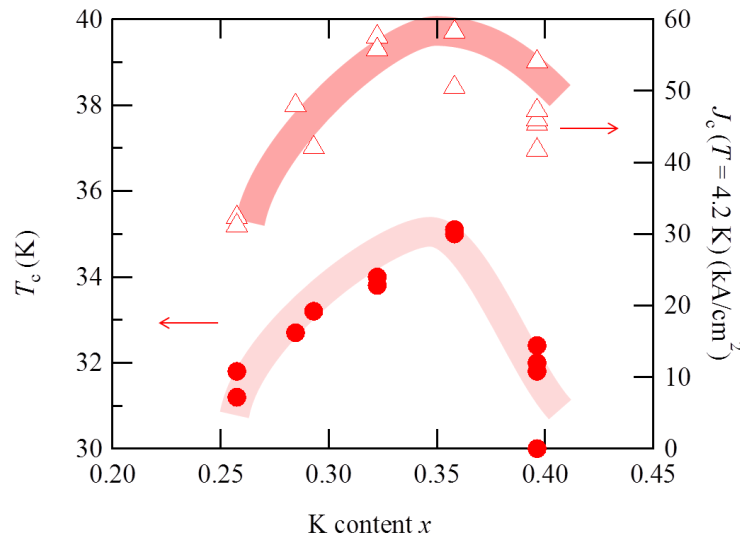


Figure 5. K content dependence of both T_c and J_c in several $Ba_{1-x}K_xFe_2As_2$ HIP wires.

4. Summary

The K content dependence of J_c in $Ba_{1-x}K_xFe_2As_2$ single crystals and HIP wires were investigated. $Ba_{1-x}K_xFe_2As_2$ single crystals are synthesized by FeAs flux method. $Ba_{1-x}K_xFe_2As_2$ HIP wires are fabricated using polycrystalline $Ba_{1-x}K_xFe_2As_2$. We found that the x -dependence of magnetic J_c in our single crystals shows the peak in under-doped region around $x \sim 0.28$. In the HIP wire, although significant peak is not observed, J_c shows a broad plateau in a wide doping region of $0.3 < x < 0.4$. These results indicate that J_c in the under-doped $Ba_{1-x}K_xFe_2As_2$ HIP wire is controlled by intergranular J_c .

Acknowledgments

This work was partially supported by a Grant-in-Aid for Young Scientists (B) (No.16K17745), the Japan-China Bilateral Joint Research Project by the Japan Society for the Promotion of Science (JSPS).

References

- [1] Ma Y 2012 *Supercond. Sci. Technol.* **25** 113001
- [2] Pallecchi I, Eisterer M, Malagoli A and Putti M 2015 *Supercond. Sci. Technol.* **28** 114005
- [3] Weiss J D, Tarantini C, Jiang J, Kametani F, Polyanskii A A, Larbalestier D C and Hellstrom E E 2012 *Nat. Mat.* **11** 682
- [4] Hecher J, Baumgartner T, Weiss J D, Tarantini C, Yamamoto A, Jiang J, Hellstrom E E, Larbalestier D C and Eisterer M 2016 *Supercond. Sci. Technol.* **29** 025004
- [5] Pyon S, Suwa T, Park A, Kajitani H, Koizumi N, Tsuchiya Y, Awaji S, Watanabe K and Tamegai T 2016 *Supercond. Sci. Technol.* **29** 115002
- [6] Pyon S, Tsuchiya Y, Inoue H, Kajitani H, Koizumi N, Awaji S, Watanabe K and Tamegai T 2014 *Supercond. Sci. Technol.* **27** 095002
- [7] Gao Z, Togano K, Matsumoto A and Kumakura H 2014 *Sci. Rep.* **4** 4065

- [8] Lin H, Yao C, Zhang X, Dong C, Zhang H, Wang D, Zhang Q, Ma Y, Awaji S, Watanabe K *et al.* 2014 *Sci. Rep.* **4** 6944
- [9] Pyon S, Yamasaki Y, Kajitani H, Koizumi N, Tsuchiya Y, Awaji S, Watanabe K and Tamegai T 2015 *Supercond. Sci. Technol.* **28** 125014
- [10] Pyon S, Taen T, Ohtake F, Tsuchiya Y, Inoue H, Akiyama H, Kajitani H, Koizumi N, Okayasu S and Tamegai T 2013 *Appl. Phys. Express* **6** 123101
- [11] Rotter M, Tegel M and Johrendt D 2008 *Phys. Rev. Lett.* **101** 107006
- [12] Sasmal K, Lv B, Lorenz B, Guloy A M, Chen F, Xue Y-Y and Chu C-W 2008 *Phys. Rev. Lett.* **101** 107007
- [13] Song D, Ishida S, Iyo A, Nakajima M, Shimoyama J, Eisterer M and Eisaki H 2016 *Sci. Rep.* **6** 26671
- [14] Kihou K, Saito T, Ishida S, Nakajima M, Tomioka Y, Fukazawa H, Kohori Y, Ito T, Uchida S, Iyo A *et al.* 2010 *J. Phys. Soc. Jpn.* **79** 124713